Photoproduction in Ultra-Peripheral Heavy-Ion Collisions

Joakim Nystrand
Department of Physics and Technology, University of Bergen, Bergen, Norway

Abstract
This presentation summarizes the results on ultra-peripheral collisions obtained at RHIC. It also discusses some aspects of the corresponding electromagnetic interactions in pp and $p\overline{p}$ collisions.

Ultra-peripheral nucleus-nucleus collisions are defined as collisions in which the distance between the nuclei is large enough that no purely hadronic interactions can occur. This roughly means impact parameters larger than the sum of the nuclear radii. The interaction is then instead mediated by the electromagnetic field. For a recent review of ultra-peripheral collisions, see [1].

1 Ultra-peripheral collisions at RHIC

The Relativistic Heavy-Ion Collider (RHIC) at Brookhaven National Laboratory began operating in the year 2000. This meant an increase in the maximum center of mass energies for heavy-ion collisions by more than an order of magnitude compared with the earlier fixed-target experiments.

At very high collision energies, the electromagnetic field surrounding a nucleus contains photons energetic enough to produce new particles in ultra-peripheral collisions. This can happen in a purely electromagnetic process through a two-photon interactions or in an interaction between a photon from one of the nuclei and the other ("target") nucleus. The photon spectrum for a minimum impact parameter, b_{min}, extends to $\sim \gamma/b_{min}$, which corresponds to about 300 GeV in the rest frame of the target nucleus in a gold on gold collision at RHIC. These photon energies are thus far above the threshold for particle production. The coherent contribution from the Z protons in the nucleus, furthermore, enhances the number of equivalent photons by a factor Z^2.

The high photon energies and fluxes lead to large cross sections for several photon-induced reactions; some have cross sections much larger than the total hadronic cross section and are major sources of beam-loss at heavy-ion colliders [2]. For example, the cross section for breaking up one of the nuclei in an Au+Au collision at RHIC through a photonuclear interaction is 95 b. The cross section for exchanging two photons and thereby simultaneously breaking up both nuclei in the same event is also large, about 4 b. The dominating fragmentation mechanism is excitation to a Giant Dipole Resonance followed by emission of one or a few neutrons.

The mutual Coulomb dissociation has been studied at RHIC by detecting the forward going neutrons in Zero-Degree Calorimeters [3]. These are located 18 m downstream from the interaction point and have an angular acceptance of $\theta < 2$ mrad with respect to the beam axis. The relative contribution of the photon-induced fragmentation to the total cross section was found to be in good agreement with calculations based on the method of equivalent photons combined with measured γ+Au cross sections. The calculations also reproduced the neutron multiplicity distribution for photon-induced events reasonably well.

Another ultra-peripheral process with very high cross section is two-photon production of electron-positron pairs. Of particular interest is the sub-class of events where the produced electron binds to one of the beam nuclei. The captured electron changes the charge and thus the rigidity of the ion, leading to a different deflection by the guiding magnets in the accelerator ring and eventual loss. Under certain conditions, the ion with an attached electron will hit the wall of the beam-pipe enclosure at a well-defined spot down stream of the interaction point. At the Large Hadron Collider at CERN, because of the high beam flux and energy, this has the potential to heat and quench the superconducting magnets near this area. The phenomenon was recently observed for the first time at RHIC with Cu–beams [4]. The location of the point of incidence ($\approx$140 m downstream from the interaction point) and the multiplicity of secondary particles resulting from the interaction of the 100 A GeV Cu beam with the beam-pipe and the surrounding magnets were found to be in good agreement with theoretical calculations, although the experimental uncertainties were large.

Particle production in ultra-peripheral collisions has been studied by both of the two large experiments at RHIC, STAR and PHENIX. Some of these results will be discussed in the following two sections.

2 Results from STAR

The first results on particle production in ultra-peripheral collisions at RHIC were studies of coherent production of ρ^0 mesons in Au+Au interaction by the STAR collaboration [5]. The cross section to produce a ρ^0 in an Au+Au collision at RHIC is about 10% of the total inelastic, hadronic cross section.

STAR has also published final results on two-photon production of free e^+e^-–pairs [6] and preliminary results on photo-production of ρ^0 in d+Au collisions [7] and coherent production of four pions in Au+Au collisions [8].

In d+Au collisions more than 90% of the photo-produced ρ^0 mesons come from events where the gold nucleus emitted the photon. The interactions can leave the deuteron intact $\gamma+d \rightarrow \rho^0+d$ or lead to break-up $\gamma+d \rightarrow \rho^0+n+p$. Two triggers were implemented to study the two cases. Both were based on triggering on low multiplicity combined with a "topology" cut to reject cosmic rays. The multiplicity was measured in the STAR Central Trigger Barrel, which consists of 240 scintillators covering the full azimuth in the pseudo-rapidity range $|\eta| < 1$. To trigger on interactions where the deuteron breaks up, it was in addition required that the forward going neutron should be detected in the Zero Degree Calorimeter. Examples of the $\pi^+\pi^-$ invariant mass distributions for the two samples are shown in Fig. 1.

The invariant mass distribution is well described by the sum of the amplitudes for a resonant ρ^0 term and a non-resonant (Söding) term:

$$\frac{d\sigma}{dm_{\pi\pi}} = \left| A\frac{\sqrt{m_{\pi\pi}m_\rho\Gamma_\rho}}{m_{\pi\pi}^2 - m_\rho^2 + im_\rho\Gamma_\rho} + B \right|^2 + f_p \qquad (1)$$

Here, $\Gamma_\rho = \Gamma_0 \cdot (m_\rho/m_{\pi\pi}) \cdot [(m_{\pi\pi}^2 - 4m_\pi^2)/(m_\rho^2 - 4m_\pi^2)]^{3/2}$ is the momentum dependent width, Γ_0 the natural width, and f_p is a second order polynomial describing the background (estimated from the like-sign yield). The mass and width of the ρ^0 are consistent with the Particle Data

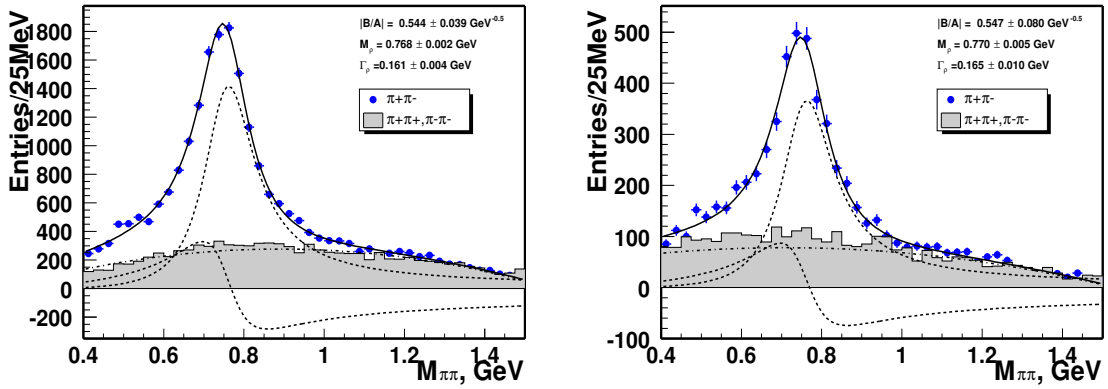

Fig. 1: Invariant mass distributions for photoproduction of $\pi^+\pi^-$–pairs in d+Au interactions at RHIC. The left (right) figure is for reactions where the deuteron remains intact (breaks up). From [7].

Group values. The ratio A/B is a measure of the relative resonant to non-resonant contribution. The values observed in d+Au interactions (0.544 and 0.547 GeV$^{-1/2}$) are consistent, within errors, with the value obtained in Au+Au interactions, $0.81 \pm 0.08 \pm 0.20$ GeV$^{-1/2}$ [5].

3 Results from PHENIX

The PHENIX experiment has studied the production of high-mass ($m_{inv} > 1.6$ GeV) e^+e^--pairs and J/Ψ mesons in ultra-peripheral Au+Au collisions [9]. A trigger was implemented for events where at least one of the nuclei break up through Coulomb dissociation. The trigger required a cluster with energy deposit $E > 0.8$ GeV in the Electromagnetic Calorimeter in coincidence with a signal in one of the Zero Degree Calorimeters and in anti-coincidence with a signal in the Beam-Beam Counters. The latter are Cherenkov counters covering $3.0 < |\eta| < 3.9$ and the absence of a signal corresponds to a rapidity gap on each side of the produced particles.

In the offline analysis, the electron and positron were identified by the Ring Imaging Cherenkov Counters and Electromagnetic Calorimeters. These detectors are part of the PHENIX mid-rapidity tracking arms and cover 2×90^o in azimuth and $|\eta| < 0.35$ in pseudo-rapidity. Signal events were defined as those events with exactly one reconstructed e^+ and one reconstructed e^- in opposite tracking arms. Events with a like-sign pair were used to estimate the amount of background.

The transverse momentum and invariant mass distributions with the background from like-sign pairs subtracted are shown in Fig. 2. The transverse momentum is here the absolute value of the vector sum of the transverse momenta of the the e^+ and e^-.

The results show that exclusive production of high-mass e^+e^--pairs in Au+Au interactions at RHIC can be understood as a continuum contribution from two-photon production $\gamma + \gamma \rightarrow e^+e^-$ and a contribution from photoproduction of J/Ψs decaying into e^+e^--pairs.

The cross section to produce a J/Ψ in a coherent interaction is much larger than the cross

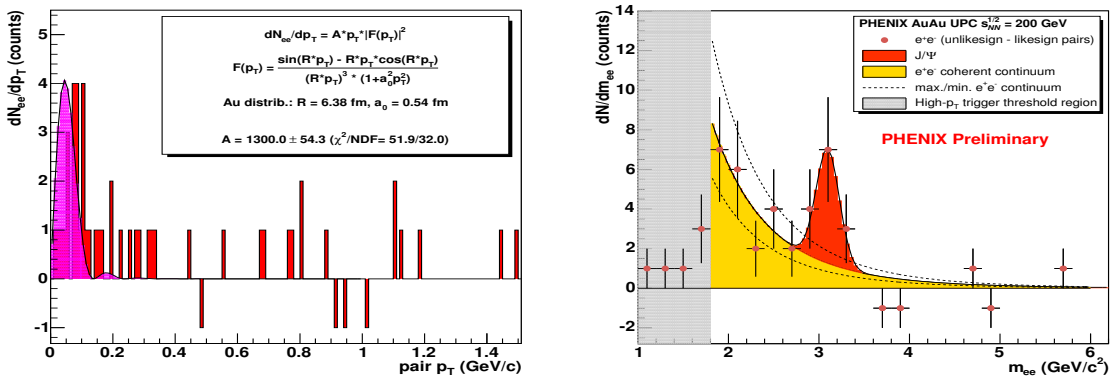

Fig. 2: Transverse momentum (left) and invariant mass (right) distributions for e^+e^--pairs produced in ultra-peripheral Au+Au collisions. The background estimated from events with like-sign pairs have been subtracted (hence the negative entries in some bins). The curve in the left figure corresponds to the nuclear form factor. The solid curve in the right figure is a fit to the sum of a continuum and J/Ψ distribution. The two additional dashed curves indicate the maximum and minimum continuum contributions. From [9].

section to produce a continuum pair in the corresponding mass range, but the branching ratio for $J/\Psi \rightarrow e^+e^-$ (5.94 %) and the broadening of the J/Ψ peak because of the limited experimental resolution make the rates comparable in the relevant mass range [10].

The transverse momentum distribution shows a clear peak at very low transverse momenta, which is expected for coherent events where the momentum transfer is restricted by the nuclear form factor. The signal events with $p_T > 100$ MeV/c are believed to come from quasi-elastic J/Ψ photoproduction, $\gamma + nucleon \rightarrow J/\Psi + nucleon$ [11].

The total net number of e^+e^--pairs in the sample (integrated luminosity $120 \pm 10\ \mu\text{b}^{-1}$) is about 40, of which ≈10 are estimated to come from decay of J/Ψs. The observed rates are in reasonable agreement with expectations for $\gamma\gamma \rightarrow e^+ + e^-$ and photoproduction of J/Ψ [10].

4 Ultra-peripheral proton-proton collisions

Electromagnetic interactions can of course also be studied with beams of protons or anti-protons, but there is then no enhancement ($\propto Z^2$) in the photon flux. Although evidence for electromagnetic particle production in pp collisions were observed at the ISR almost 30 years ago [12], electromagnetic interactions in pp collisions have so far attracted relatively little attention, much less than particle production in doubly diffractive interactions, for example. The CDF Collaboration has, however, recently published its first paper on two-photon production of e^+e^-–pairs with $m_{inv} > 10$ GeV in $p\overline{p}$ collisions at the Tevatron [13].

The choice of minimum invariant mass is unfortunate, since it falls right in the range of the $\Upsilon(1S)$, $\Upsilon(2S)$, and $\Upsilon(3S)$ vector mesons, and, as will be shown, these vector mesons are expected to give a significant contribution to the exclusive production of e^+e^-–pairs through the decay $\Upsilon \rightarrow e^+e^-$.

CDF is also analyzing the exclusive production of $\mu^+\mu^-$–pairs, $p\overline{p} \rightarrow p\overline{p} + \mu^+\mu^-$, at

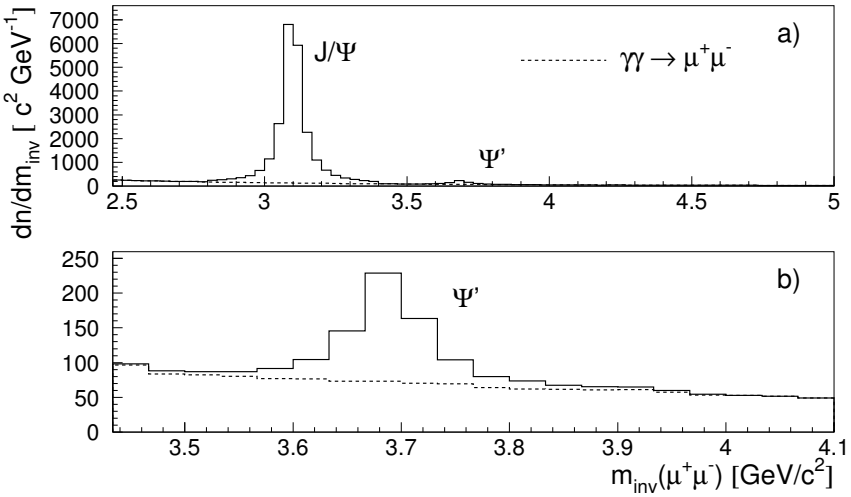

Fig. 3: Calculated invariant mass distributions for electromagnetic production of $\mu^+\mu^-$–pairs around mid-rapidity ($|\eta| < 2$) in $\sqrt{s}$ = 1.96 TeV $p\overline{p}$ collisions. Figure b) shows the same distribution as a) but restricted to a narrow intervall around the Ψ' mass. The widths of the J/Ψ and Ψ' have been set to roughly correspond to typical experimental widths.

lower invariant masses [14]. The two main contributions to these events are, as with heavy-ion beams, $\gamma\gamma \rightarrow \mu^+ + \mu^-$ and γ+Pomeron $\rightarrow J/\Psi$ or Ψ', followed by decay of the vector meson to a dilepton pair. There could also be a contribution from the elusive Odderon through the reaction Odderon+Pomeron $\rightarrow V \rightarrow \mu^+ + \mu^-$ [15, 16]. The size of this contribution is not very well known; it is possible that it is comparable to the other two processes.

There could also be a background to the J/Ψ production from Pomeron+Pomeron interactions producing a χ_c via the decay $\chi_c \rightarrow J/\Psi + \gamma$ where the photon escapes detection. This background is a problem only for the J/Ψ and not for the Ψ'.

Figure 3 shows the calculated yields for continuum $\mu^+\mu^-$–production and photoproduction of J/Ψ and Ψ' followed by decay to $\mu^+\mu^-$–pairs for $p\overline{p}$ collisions at the Tevatron ($\sqrt{s}$ = 1.96 TeV). It is required that both muons are within $|\eta| < 2$ to simulate the typical experimental acceptance at high-energy colliders. The vector meson production is calculated as in [17], but with a larger cut-off for the minimum impact parameter ($b > 1.4$ fm rather than 0.7 fm). This is believed to better reproduce the condition of no accompanying hadronic interactions. The input $\gamma + p \rightarrow p + \Psi'$ cross section is taken from [18]. The continuum $\gamma + \gamma \rightarrow \mu^+\mu^-$ is calculated under the same conditions as the vector mesons. The contribution from two-photon interactions is much smaller in pp or $p\overline{p}$ collisions compared with in heavy-ion collisions (cf. Fig. 2). The calculated cross sections are given in Table 1.

Table 1: Cross sections for photoproduction of vector mesons and $\mu^+\mu^-$–pairs in $p\overline{p}$ collisions at the Tevatron ($\sqrt{s}$ = 1.96 TeV). The rightmost column shows the cross section multiplied with the branching ratio for decay into $\mu^+\mu^-$.

	σ [nb]	$\sigma \cdot Br(\mu^+\mu^-)$ [nb]
$p + \overline{p} \rightarrow p + \overline{p} + J/\Psi$	15	0.87
$p + \overline{p} \rightarrow p + \overline{p} + \Psi'$	2.4	0.018
$p + \overline{p} \rightarrow p + \overline{p} + \mu^+\mu^-$ ($m_{inv} > 1.5$ GeV)	2.4	2.4

5 Summary

The fact that particles are produced in ultra-peripheral collisions and that the experiments that were designed to study central collisions can detect them have been shown by the STAR and PHENIX experiments at RHIC. Hopefully, the increase in the cross sections with energy and the extended trigger capabilities of future experiments will lead to an increased interest for ultra-peripheral collisions in proton-proton and heavy-ion collisions at the Large Hadron Collider.

References

[1] C. Bertulani, S. Klein, and J. Nystrand, Ann. Rev. Nucl. Part. Sci. **55**, 271 (2005).

[2] A. Baltz, M. Rhoades-Brown, and J. Weneser, Phys. Rev. E **54**, 4233 (1996).

[3] M. Chiu *et al.*, Phys. Rev. Lett. **89**, 012302 (2002).

[4] R. Bruce *et al.*, Phys. Rev. Lett. **99**, 144801 (2007).

[5] STAR Collaboration, C. Adler *et al.*, Phys. Rev. Lett. **89**, 272302 (2002).

[6] STAR Collaboration, J. Adams *et al.*, Phys. Rev. C **70**, 031902 (2004).

[7] STAR Collaboration, S. Timoshenko *et al.*, nucl-ex/0501010.

[8] STAR Collaboration, S. Klein *et al.*, nucl-ex/0506013.

[9] PHENIX Collaboration, D. d'Enterria *et al.*, nucl-ex/0601001 (Presentation at Quark Matter 2005).

[10] J. Nystrand, Nucl. Phys. A **752**, 470 (2005).

[11] M. Strikman, M. Tverskoy, and M. Zhalov, Phys. Lett. B **626**, 72 (2005).

[12] F. Vanucci *et al.*, CERN-EP/80-82, available from http://cdsweb.cern.ch/.

[13] CDF Collaboration, A. Abulencia *et al.*, Phys. Rev. Lett. **98**, 112001 (2007).

[14] A. Hamilton, private communication.

[15] L. Szymanowski, these proceedings.

[16] A. Schäfer, L. Mankiewicz, and O. Nachtmann, Phys. Lett. B **272**, 419 (1991).

[17] S. Klein and J. Nystrand, Phys. Rev. Lett. **92**, 142003 (2004).

[18] H1 Collaboration, C. Adloff *et al.*, Phys. Lett. B **541**, 251 (2002).